Engineering the structure-induced enhanced absorption in three-dimensional metallic photonic crystals

Hong-Yi Sang and Zhi-Yuan Li*
Institute of Physics, Chinese Academy of Sciences, P. O. Box 603, Beijing 100080, China

Ben-Yuan Gu
CCAST (World Laboratory), P.O. Box 8730, Beijing 100080, China
and Institute of Physics, Chinese Academy of Sciences, P.O. Box 603, Beijing 100080, China
(Received 29 July 2004; published 10 December 2004)

Order-of-magnitude enhancement of light absorption can take place near the photonic band gaps in three-dimensional layer-by-layer metallic photonic crystals in the mid-infrared wavelength regime where a conventional bulk metallic material shows weak absorption. In this paper we investigate the dependence of this enhanced absorption on several structural parameters of the crystal by means of a plane-wave-based transfer-matrix method in combination with an analytic model expansion approach. We find that when the metallic layers are brought out of touch, the magnitude of the absorption peaks grows rather than decays, in contrast with the conventional wisdom that the connectivity of metallic structure can enhance the absorption. Besides, the increase in the metallic layer separation distance will result in redshifts of absorption peak. The position of the absorption peak can also be engineered conveniently by simply changing the refractive index of the dielectric material filling the open domain between metal walls. Due to the approximate scalability of Maxwell's equations, the absorption peak shows a nearly linear dependence in position on this refractive index.

DOI: 10.1103/PhysRevE.70.066611 PACS number(s): 42.70.Qs, 41.20.Jb, 78.70.Gq

I. INTRODUCTION

In recent years, complex three-dimensional (3D) metallic photonic crystal (MPC) structures have raised great interest owing to their potential applications in many high technology areas such as filters and polarizers in the microwave wavelength, beam splitters and mirrors in the infrared regime [1–19]. Compared with their dielectric counterparts [1,2], MPC's have a greatly enhanced contrast in the dielectric constant of the composite materials, and as a result possess to a larger photonic band gap [3–10]. Very recently, Lin and coworkers have successfully fabricated high-quality 3D MPC's working in the infrared wavelengths by means of state-of-the-art lithographic techniques under a layer-by-layer fabrication scheme [11–15]. Promising experimental data have demonstrated that these metallic microstructures can be useful for incandescent lamp application and for thermal photovoltaic power generation. Theoretical analysis has shown that the existence of photonic band gaps and modification of the photon density of states in these MPC's can lead to significant enhancement of thermal radiation at a narrow frequency window around the band gap [16–20]. Such theoretical and experimental works have opened a new frontier for the MPC's to be used in the high temperature regime.

It has been well known that metals in their bulk material form exhibit small absorption in the mid-infrared wavelength regime. For instance, a tungsten thin film has an absorption coefficient below 2% at around 4 μm. However, when metallic materials are brought into the form of microstructures such as 3D layer-by-layer photonic crystals, there can be order-of-magnitude enhancement of absorption due to the existence of photonic band gaps in these microstructures [16–18]. Previous theoretical analysis and numerical simulations over the ordinary layer-by-layer MPC's have shown that the enhanced absorption peaks are located close to both the band gap edge and the high transmission pass band, and this absorption peak can be deep below the conventional metallic waveguide cutoff frequency when there exists a significant global coupling effect between different metallic layers [16,17]. In Ref. [16], the effect of the metallic layer thickness on the magnitude and position of the absorption peaks was investigated. In this paper we will further examine from the theoretical side the dependence of the structure-induced enhancement of absorption on other structural parameters in an MPC that is similar to but more general than the ordinary layer-by-layer MPC [11–18].

The remaining part of this paper is arranged as follows. In Sec. II we first briefly describe the procedure of our theoretical approach, which is basically the combination of the plane-wave-based transfer-matrix method and the analytic modal solution approach. We then use this approach to investigate the effect of the separation distance between metallic layers and the separation materials, as well as the materials filling the open domain between metal walls in each layer on the absorption of electromagnetic (EM) waves in the new general MPC structures. Such knowledge allows one to have a deeper understanding about the physical origin of this structure-induced enhancement of absorption. In Sec. III we will present a brief summary to this paper.

II. RESULTS AND DISCUSSIONS

The basic geometric configuration of a usual 3D laer-by-layer MPC is schematically depicted in Fig. 1(a). The MPC

*Electronic address: lizy@aphy.iphy.ac.cn

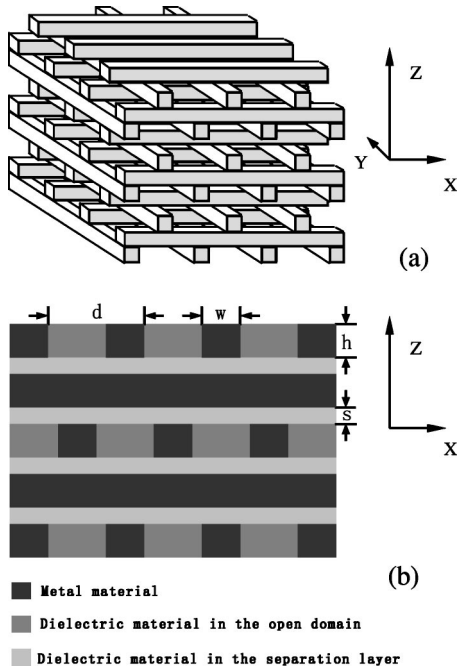

FIG. 1. (a) Schematic configuration of an ordinary 3D layer-by-layer MPC composed of rectangular tungsten rods. The primitive unit cell is arrayed into an face-centered-tetragonal lattice. (b) The picture of cross section vertical to the (010) direction of the general MPC's under study in the paper. The space between the adjacent rods, the width and thickness of each rod, and the separation space between two metallic layers are represented by d, w, h, and s.

is stacked from rectangular metallic rods which are arrayed in a face-centered-tetragonal lattice. The stacking direction is set to be the (001) direction, which is parallel to the z axis. This metallic structure can be built by infiltration of metallic materials into an original template, which is also a layer-by-layer photonic crystal but made from dielectric materials such as silicon [11–15]. The adjacent metallic layers are in touch with each other and the open domain between the metal walls in each layer is an air background. The MPC we consider in this paper is similar to the ordinary layer-by-layer MPC but has a more general configuration and allows additional structural freedoms to be incorporated to adjust the optical properties. The geometry of the new MPC is schematically depicted in Fig. 1(b) for the cross sectional picture in the (010) plane. The open domain between the metallic walls now might be filled with a general homogeneous dielectric material whose refractive index is n_f. A homogeneous thin film is introduced as a separation layer between adjacent metallic layers. The thin film has a thickness s and refractive index of n_s. The usual layer-by-layer MPC can be assumed to be a special case of the new MPC with parameters of $n_f=1$, $s=0$, and $n_s=1$.

The theoretical approach for solving light propagation through the general MPC is close to that for an ordinary layer-by-layer MPC. For such microstructures that are made from highly conducting metallic materials and operate in the mid-infrared wavelength regime, the basic theoretical tool is the plane-wave-based transfer-matrix method in combination with the analytic modal solution approach. In brief, one first finds out the solution of the EM eigenmodes within each metallic layer by means of an analytical manipulation. This is possible because each metallic layer is a 1D lamellar grating [18,24–29]. Such an analytical step proves to be the key to the high efficiency of the whole theoretical scheme as the eigenmodes have already accurately accounted for the small skin depth of metal, which is two orders of magnitude smaller than the incident wavelength. The next step is to project these eigenmodes onto the plane-wave function space associated with the eigenmodes of EM fields in an air background. From this the transfer matrix (such as the scattering matrix) for the metallic layer on the plane-wave basis can be built. The same procedure holds for all the four metallic layers in each unit cell, but a simpler and more efficient way is to utilize the translational and rotational symmetries between these layers. The transfer matrix for a homogeneous dielectric thin film can also be derived analytically. With these individual transfer matrices at hand, the last thing is to construct the overall transfer matrix for a unit cell and then a slab consisting of multiple unit cells, based on which all interesting physical quantities such as the transmission, reflection, and absorption spectra for the metallic MPC can be extracted. More details of the theoretical approaches can be referred to Refs. [18,21–23].

The periodic array of metallic rods can be regarded as forming the principal skeleton of the MPC structure. It shapes the basic optical properties of the MPC, such as the existence of a long-wavelength stop band gap due to the conventional waveguide cutoff, and the enhancement of absorption induced by the microstructure of metal. In our simulations, we assume that this metal skeleton is made from tungsten and has fixed geometrical parameters as: the spacing between two adjacent rods is $d=4.2$ μm, and each rod has width $w=4.2$ μm and thickness $h=1.5$ μm. Besides, the sample is four layers (namely, one unit cell) thick. On the other hand, the dielectric part can modify the behavior of wave propagation in the metallic skeleton, so much as to determine, for instance, the precise position of the lowest pass band, higher band gaps and absorption peaks, and the degree of structure-induced enhancement of the absorption on EM radiations. Investigation on the role played by the dielectric materials may help to reveal the origin of the enhanced absorption in the MPC's.

We first look at the transmission, reflection, and absorption spectra for the ordinary layer-by-layer MPC sample, namely, $s=0$, $n_f=1$, and $n_s=1$. This MPC has been discussed both experimentally and theoretically [11,16–18]. The calculation results are reproduced and plotted in Fig. 2(a) for the sake of reference. Here we have considered normal incidence of unpolarized plane waves. To achieve this, we consider incidence of two independent plane waves that are orthogonally polarized (one with the electric field parallel to the rod in the top layer and the other perpendicular) and have equal intensity. A high reflection and low transmission range appears above the wavelength of about 6 μm, which is recognized to be the stop band gap. This size is close to the conventional waveguide cutoff wavelength, which is about twice the open domain size (3.0 μm). Below this wavelength, a wide high-transmission band stands out with the longer-wavelength peak located at about 5.6 μm. The most distin-

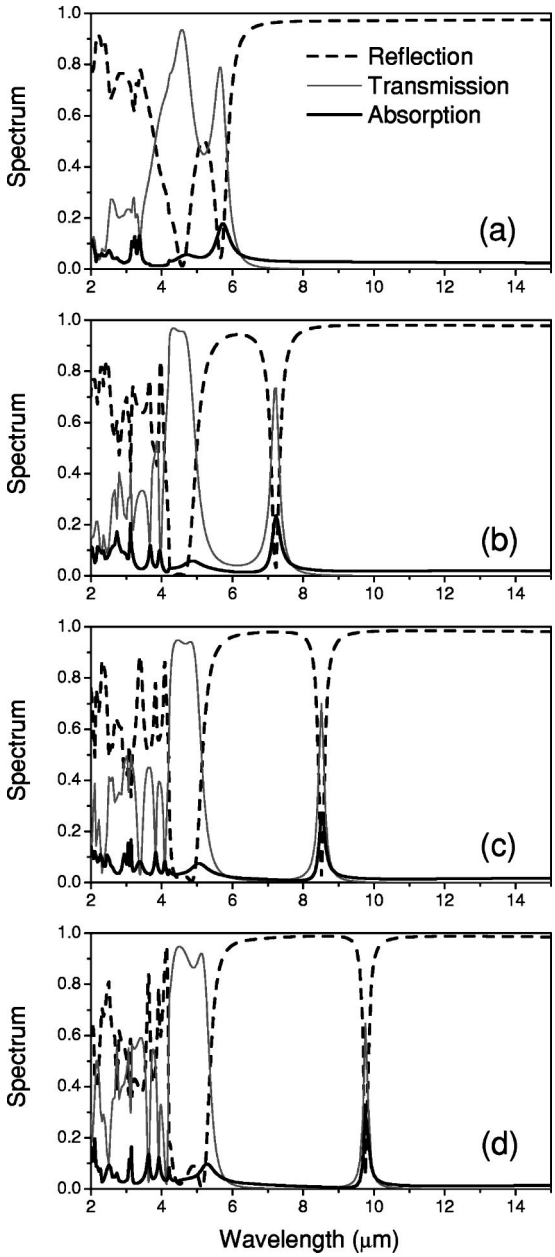

FIG. 2. Calculated optical spectra of the MPC samples with different thicknesses of the separation air film as (a) $s=0$, (b) $s=0.2h$, (c) $s=0.4h$, and (d) $s=0.6h$. The open domain within each metallic layer is an air background.

guished feature is a sharp absorption peak located at about 5.7 μm (close to both the transmission peak and the stop band edge) with a magnitude of about 19%, which is one order of magnitude larger than the absorption coefficient of a bulk tungsten (say, a homogeneous tungsten thin film) at the same wavelength, in consistence with the experimental data [11]. This absorption enhancement has been ascribed to two dominant mechanisms: The slow down of EM wave propagation near the band gap (small group velocity) and the presence of a high transmission band at the same wavelength [16–18]. Both mechanisms increase the flow of EM wave through the whole metallic structure, and thus enhance the absorption.

Due to the structural similarity to the ordinary layer-by-layer MPC's, it can be expected that the enhanced absorption should also exist in the new general MPC's under the same physical mechanisms. In our first step, we bring metallic rods that are originally in connection along the (001) direction out of touch. The calculated transmission, reflection, and absorption spectra for increasing separation distances as $s=0.2h$, $0.4h$, and $0.6h$ are displayed in Figs. 2(b)–2(d), respectively. It can be seen that the order-of-magnitude enhancement of absorption take place in all MPC's compared with an unstructured tungsten bulk material. The dominant absorption shows up in the lowest absorption peak, and the peak redshifts from 5.7 μm for the ordinary MPC (with $s=0$) to 7.2, 8.5, and 9.8 μm, respectively, for the above three MPC's. Similar phenomenon of redshift has been observed in the ordinary layer-by-layer MPC when the thickness of each metallic layer increases. The reason can be attributed to the appearance of a new pass band within the long-wavelength stop gap which is primarily induced by the conventional metallic waveguide cutoff effect [16]. That this assumption is reasonable can be seen from the existence of the long-wavelength transmission peaks in Fig. 2 below the cutoff wavelength of 6 μm. The pass band shifts to a longer wavelength for a larger air-film separation distance and therefore a larger lattice constant in the (001) direction. In addition, the band width becomes increasingly narrower. As a result, the group velocity of wave along the (001) direction slows down, leading to enhancement of absorption. This is clearly reflected in Figs. 2(a)–2(d) from an increasingly sharper absorption peak which almost overlaps in frequency with the transmission peaks (and reflection dips) and whose maximum magnitude monotonously grows from 19% to 23%, to 27%, and to 32%, although the total thickness of the metallic domain keeps unchanged. It is obvious that the two physical mechanisms for the ordinary layer-by-layer MPC's also play a key role in shaping the absorption characteristic of the new MPC's.

The above observation that the absorption of EM waves enhances when the metallic rods are brought out of touch each other is somewhat beyond our expectation. The conventional wisdom holds that the connectivity of metal structures can offer channels for surface currents that are induced by external EM wave radiations to flow in the whole metallic structure, and therefore increases the loss of absorption. This is a well-known fact for electric direct current transport in metal wires. Probably for this reason, it has been suggested that the absorption loss should be significantly reduced in an opal-based MPC made from metallic spherical particles when the metal particle is coated with a thin film of polymer to form a separation layer [30,31]. In this context, it is a little bit surprising to find the inverse absorption behavior that isolation of metal structures does not reduce, but increases the absorption. The possible reason for this anomalous phenomenon might be the difference in the transport mechanism between EM waves and electric direct currents. The latter strongly depends on the connectivity of metal structures, while the former can transport without the help of a medium. Besides, a separation layer might facilitate the coupling between surface plasmons that are excited in different metal rods and leads to a stronger absorption effect.

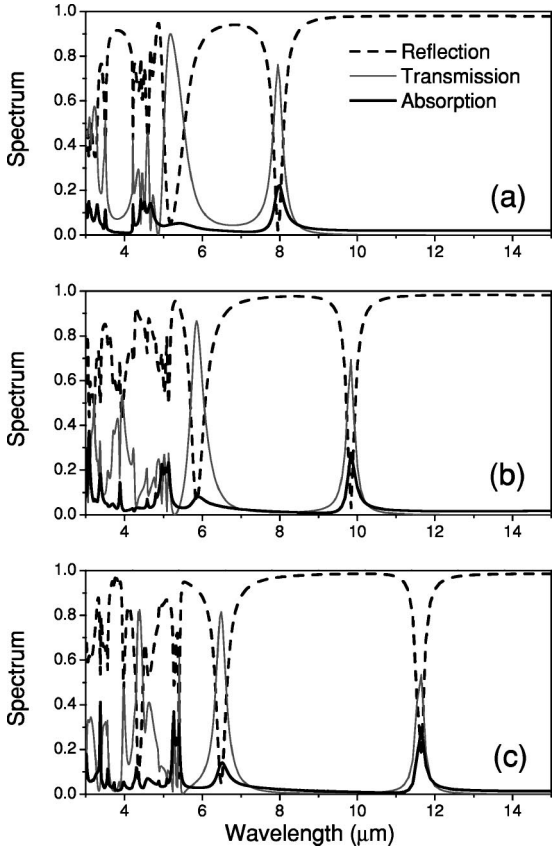

FIG. 3. Calculated optical spectra of the MPC samples with different thicknesses of the separation silica film as (a) $s=0.2h$, (b) $s=0.4h$, and (c) $s=0.6h$. The open domain within each metallic layer is an air background.

In our next step we consider MPC's where the air-film separation layers in Fig. 2 are replaced by silica layers. The calculation results of the optical spectra are displayed in Fig. 3 for three cases of layer thickness as (a) $s=0.2h$, (b) $s=0.4h$, and (c) $s=0.6h$. The open domain in each metallic layer is still an air background. The overall characteristic of the spectra is similar to the air-film MPC's, in particular, an order-of-magnitude enhancement of absorption is also observed in all MPC's. Compared with the air-film sample, the dominant absorption peak in the silica-film sample now further shifts to longer wavelengths at 8.0, 9.9, and 11.6 μm, respectively. The maximum absorption coefficient witnesses a slight reduction and assumes a value of 22%, 27%, and 29% for the three MPC samples. The redshifts of the dominant absorption peak can be understood by noticing that the silica film increases the light path of EM waves in the (001) direction due to a refractive index growth, and thus the equivalent lattice constant in this direction.

Apart from changing the (001) lattice constant by introducing a separation thin film into the ordinary layer-by-layer MPC, the absorption band can be engineered by modifying the open domain within each metallic layer, for instance, changing the filling dielectric materials. This scheme has a practical advantage over the above two schemes because in experiment it is easier to fill dielectric materials into an existing MPC template than fabrication of a new MPC through

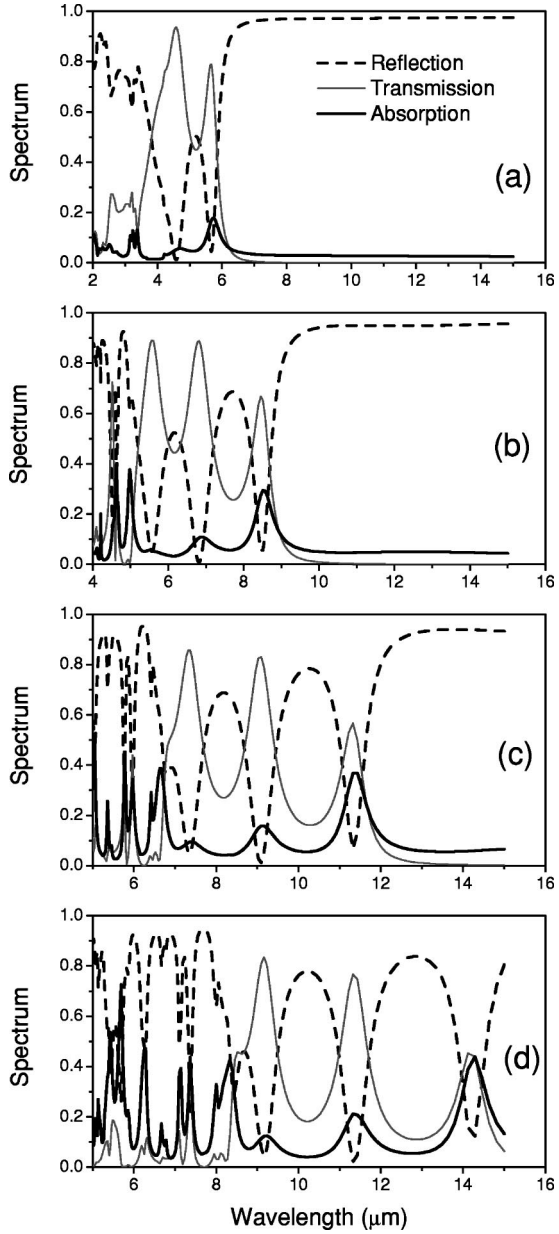

FIG. 4. Calculated optical spectra of the MPC samples with the separation space $s=0$. The open domain between metallic walls in each layer are filled with dielectric materials of different refractive indices as (a) $n_f=1$, (b) $n_f=1.5$, (c) $n_f=2$, and (d) $n_f=2.5$.

time-consuming lithographic techniques. In Fig. 4, we plot the optical spectra of MPC samples with the separation space $s=0$. The open domain between metallic walls are filled with dielectric materials of different refractive indices as (b) $n_f=1.5$, (c) $n_f=2$, and (d) $n_f=2.5$. For clarity of reference, we also show the optical spectra for the ordinary layer-by-layer MPC (with $n_f=1$) in Fig. 4(a). With n_f increasing gradually, some interesting spectrum features can be seen from the figures. First, the lowest band gap edge moves to longer wavelength, from $\lambda_1=5.7$ μm, to $\lambda_2=8.5$ μm, $\lambda_3=11.4$ μm, and $\lambda_4=14.3$ μm. Almost overlapping with this band gap edge is a pass band with a significantly large transmission coefficient and a greatly enhanced absorption peak whose maximum magnitude increases from 19.0% to 29.2%, 36.4%, and

43.6%. This tendency of redshift of the absorption peak is similar to those found in Figs. 2 and 3 when the (001) lattice constant is increased.

The position of the pass band and the absorption peak for different filling dielectric materials can be well understood by noticing that the layer-by-layer metallic skeleton shapes the basic transport behavior of EM waves. This metallic skeleton, with all metal rods interconnected with each other, form a low-frequency filter to incident waves, and can block long-wavelength radiation with arbitrary polarizations. The open domain in each unit cell of the MPC, with metallic wall surrounding the four sides, behaves like a metallic square waveguide. Therefore there exists a fundamental stop band gap that can be regarded as originating from the conventional waveguide cutoff effect. The cutoff wavelength λ_{off} is fundamentally determined by the geometrical size of the open domain by a relation of $\lambda_{off} \approx 2a_{min}n_f$, where a_{min} is the side length of the open domain, which is 3 μm for the MPC here. For this reason, one can expect that the gap edge position λ_c should nearly scale proportional to the refractive index of the filling material. Surprisingly, we indeed find that the stop band gap edge of the above four MPC samples satisfy the following proportional relations: $\lambda_2/\lambda_1 \sim 1.5$, $\lambda_3/\lambda_1 \sim 2$, and $\lambda_4/\lambda_1 \sim 2.5$. This observation indicates that the formation of the lowest band gap in the current MPC's has a close connection with the metallic waveguide cutoff effect.

Another significant feature that can be found from the optical spectra in Fig. 4 is the appearance of additional absorption peaks that is associated with the high-transmission pass bands when n_f increases from 1 to 2.5. In Fig. 1(a), there appears a small bump in the shoulder of the dominant absorption peak. The position of this weak absorption peak is about 4.6 μm and the magnitude is about 5%. When n_f increases to 1.5, this second higher absorption peaks becomes quite apparent. The position shifts to about 6.9 μm and the magnitude grows to about 10.7%. When n_f further increases to 2.0 and 2.5, the absorption peak continues to redshift to 9.1 and 11.4 μm, and the maximum magnitude grows to 15.5% and 20.6%, respectively. Similar behavior can be found for the other higher absorption peaks. Physically, the appearance of new pass bands can be attributed to the increased guided mode number that a metallic waveguide can support when the refractive index n_f increases. Increasing n_f means reduced wavelength within the material or equivalently larger waveguide dimensions. On the other hand, a larger n_f also increases the path that the EM wave witnesses when it transports along the (001) direction, and therefore more waves are absorbed.

A closer look at the optical spectrum in Fig. 4 shows that not only the lowest-frequency dominant absorption peak, but also the other higher absorption peaks nearly follows the linear scaling law with respect to the refractive index of the filling materials. For instance, the position of the second higher absorption peak at the four MPC samples, which is about 4.6, 6.9, 9.1, and 11.4 μm, obviously is nearly linear with the corresponding refractive index, which is 1.0, 1.5, 2.0, and 2.5, respectively. From the mathematical point of view, such a scaling law is consistent with the approximate scalability of Maxwell's equations for a highly conducting metallic structure with respect to the refractive index of the background dielectric medium. To see this more clearly, look at the wave equation for the MPC: $\nabla \times \nabla \times \mathbf{E} - \epsilon(\mathbf{r}) k_0^2 \mathbf{E} = \mathbf{0}$, where k_0 is the wave number. The dielectric function $\epsilon(\mathbf{r})$ is ϵ_m in the metal domain and $\epsilon_f = n_f^2$ in the open domain. The wave equation can be written in another way: $\nabla \times \nabla \times \mathbf{E} - [\epsilon(\mathbf{r})/\epsilon_f](n_f k_0)^2 \mathbf{E} = \mathbf{0}$. As the metal has a very large value of ϵ_m, $\epsilon(\mathbf{r})/\epsilon_f$ can be assumed to be approximately the dielectric function for the MPC with an air background. But now all relevant physical sizes, including the absorption wavelength, have a new scale that is n_f times the original ones. In its extreme case, such a scalability should be satisfied rigorously for a perfectly conducting structure, such as a microwave metallic waveguide. From this point of view, it is not surprising to observe the redshift of the absorption peaks whose positions are nearly proportional to the refractive index of the filling material.

The above discussions have clearly shown that the propagation behavior of EM waves can be significantly altered in a microstructured 3D metallic photonic crystal. As a result, order of magnitude enhancement of absorption can be achieved. Previous works [32–34] have shown that a simple 1D metallodielectric photonic crystal made from periodic stacks of alternating metallic and dielectric thin films can also radically modify the way by which EM waves used to transport in metallic materials. For instance, Scalora and coworkers have shown that deliberately designed metallodielectric multilayer thin films can become transparent to visible or infrared light despite a total thickness of metal films far larger than the skin depth of the metal, because of a resonant tunneling effect [32,33]. It might then be possible to also attain a significant enhancement of absorption in a selective wavelength window in the optical regimes by means of such simple 1D multilayer structures. These structures are much easier to fabricate than the 3D metallic photonic crystals and thus might prove useful in application to high-performance thermal radiation devices.

III. CONCLUSIONS

In summary, we have used an efficient theoretical formulation which combines the plane-wave-based transfer-matrix method and the analytical modal solution approach to analyze the optical properties of 3D MPC's that are similar to but have more general structural configurations than the ordinary layer-by-layer MPC's, which recently have been successfully fabricated via advanced lithographic techniques and can have potential high-temperature applications. Although in the mid-infrared wavelength regime, metal in its bulk material form shows weak absorption to EM wave radiation, it can exhibit order of magnitude enhancement of absorption when it is brought into microstructures such as a photonic crystal. Two basic physical mechanisms dominantly contribute to this enhancement, one is the small group velocity of waves near the band gap edge, the other is the overlap of the absorption peak with the high-transmission pass band supported by the MPC.

We have systematically investigated the dependence of the enhanced absorption effect on several geometrical parameters of the general MPC's. We find that when the metal-

lic layers are brought out of touch and a dielectric thin film is introduced as the separation layer, the magnitude of the absorption peaks grows rather than decays. This is in contrast with the conventional wisdom that the connectivity of metallic structures can enhance the absorption. Besides, the increase in the metallic layer separation distance will result in a redshift of the absorption peak. The position and magnitude of the absorption peak can also be engineered conveniently by simply changing the refractive index n_f of the dielectric material filling the open domain between metal walls. It is found that the absorption peak approximately follows a linear relation in its position with n_f. The fundamental reason for this linearity is due to the scalability of Maxwell's equations for a highly conducting MPC with respect to n_f. These systematic examinations about the enhancement of EM wave absorption could be useful for engineering and designing MPC's that exhibit excellent optical properties associated with the high-temperature application, such as high-efficiency thermal radiation source.

ACKNOWLEDGMENTS

This work was supported by the National Key Basic Research Special Foundation of China at No. 2004CB719804 and the National Natural Science Foundation of China at No. 10404036.

[1] E. Yablonovitch, Phys. Rev. Lett. **58**, 2059 (1987).
[2] J. D. Joannopoulos, R. D. Meade, and J. N. Winn, *Photonic Crystals* (Princeton University Press, Princeton, NJ, 1995).
[3] E. R. Brown and O. B. MacMahon, Appl. Phys. Lett. **67**, 2138 (1995).
[4] M. Sigalas, C. T. Chan, K. M. Ho, and C. M. Soukoulis, Phys. Rev. B **52**, 11 744 (1995).
[5] D. F. Sievenpiper, M. E. Sickmiller, and E. Yablonovitch, Phys. Rev. Lett. **76**, 2480 (1996).
[6] S. Fan, P. R. Villeneuve, and J. D. Joannopoulos, Phys. Rev. B **54**, 11 245 (1996).
[7] E. Özbay, B. Temelkuran, M. Sigalas, G. Tuttle, C. M. Soukoulis, and K. M. Ho, Appl. Phys. Lett. **69**, 3797 (1996).
[8] S. Gupta, G. Tuttle, M. Sigalas, and K. M. Ho, Appl. Phys. Lett. **71**, 2412 (1997).
[9] I. El-Kady, M. M. Sigalas, R. Biswas, K. M. Ho, and C. M. Soukoulis, Phys. Rev. B **62**, 15 299 (2000).
[10] W. Y. Zhang, X. Y. Lei, Z. L. Wang, D. G. Zheng, W. Y. Tam, C. T. Chan, and P. Sheng, Phys. Rev. Lett. **84**, 2853 (2000).
[11] J. G. Fleming, S. Y. Lin, I. El-Kady, R. Biswas, and K. M. Ho, Nature (London) **417**, 52 (2002).
[12] S. Y. Lin, J. Moreno, and J. G. Fleming, Appl. Phys. Lett. **83**, 380 (2003).
[13] S. Y. Lin, J. G. Fleming, and I. El-Kady, Appl. Phys. Lett. **83**, 593 (2003).
[14] S. Y. Lin, J. G. Fleming, and I. El-Kady, Opt. Lett. **28**, 1683 (2003).
[15] S. Y. Lin, J. G. Fleming, and I. El-Kady, Opt. Lett. **28**, 1909 (2003).
[16] Z. Y. Li, I. El-Kady, K. M. Ho, S. Y. Lin, and J. G. Fleming, J. Appl. Phys. **93**, 38 (2003).
[17] S. Y. Lin, J. G. Fleming, Z. Y. Li, I. El-Kady, R. Biswas, and K. M. Ho, J. Opt. Soc. Am. B **20**, 1538 (2003).
[18] Z. Y. Li and K. M. Ho, Phys. Rev. B **67**, 165104 (2003).
[19] G. von Freymanna, S. John, M. Schulz-Dobrick, E. Vekris, N. Tetreault, S. Wong, V. Kitaev, and G. A. Ozin, Appl. Phys. Lett. **84**, 224 (2004).
[20] Z. Y. Li, Phys. Rev. B **66**, 241103 (2002).
[21] L. L. Lin, Z. Y. Li, and K. M. Ho, J. Appl. Phys. **94**, 811 (2003).
[22] Z. Y. Li and L. L. Lin, Phys. Rev. E **67**, 046607 (2003).
[23] Z. Y. Li and K. M. Ho, Phys. Rev. B **68**, 245117 (2003).
[24] J. R. Andrewartha, J. R. Fox, and I. J. Wilson, Opt. Acta **26**, 69 (1979).
[25] L. C. Botten, M. S. Craig, R. C. McPhedran, J. L. Adams, and J. R. Andrewartha, Opt. Acta **28**, 1087 (1981).
[26] L. C. Botten, M. S. Craig, and R. C. McPhedran, Opt. Acta **28**, 1103 (1981).
[27] P. Sheng, R. S. Stepleman, and P. N. Sanda, Phys. Rev. B **26**, 2907 (1982).
[28] S.-E. Sandström, G. Tayeb and R. Petit, J. Electromagn. Waves Appl. **7**, 631 (1993).
[29] G. Tayeb and R. Petit, Opt. Acta **31**, 1361 (1984).
[30] Z. Wang, C. T. Chan, W. Zhang, N. Ming, and P. Sheng, Phys. Rev. B **64**, 113108 (2001).
[31] A. Moroz, Phys. Rev. B **66**, 115109 (2002).
[32] M. Scalora, M. J. Bloemer, A. S. Pethel, J. P. Dowling, C. M. Bowden, and A. S. Manka, J. Appl. Phys. **83**, 2377 (1998).
[33] M. J. Bloemer and M. Scalora, Appl. Phys. Lett. **72**, 1676 (1998).
[34] R. S. Bennink, Y. K. Yoon, R. W. Boyd, and J. E. Sipe, Opt. Lett. **24**, 1416 (1999).